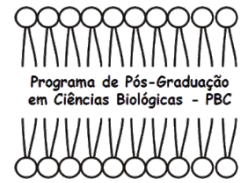




UNIVERSIDADE ESTADUAL DE MARINGÁ
CENTRO DE CIÊNCIAS BIOLÓGICAS
PROGRAMA DE PÓS-GRADUAÇÃO EM CIÊNCIAS
BIOLÓGICAS
ÁREA DE CONCENTRAÇÃO EM BIOLOGIA CELULAR E
MOLECULAR



RAÍSSA BENAN ZARA

**INVESTIGAÇÃO DA ATIVIDADE ANTITUMORAL DE COMPOSTOS
HETEROCICLICOS DE NITROGÊNIO EM LINHAGEM CELULAR DE
CÂNCER DE PRÓSTATA**

Maringá
2018

RAÍSSA BENAN ZARA

**INVESTIGAÇÃO DA ATIVIDADE ANTITUMORAL DE COMPOSTOS
HETEROCICLICOS DE NITROGÊNIO EM LINHAGEM CELULAR DE
CÂNCER DE PRÓSTATA**

Dissertação apresentada ao Programa de Pós-Graduação em Ciências Biológicas (área de concentração - Biologia Celular e Molecular), da Universidade Estadual de Maringá para a obtenção do grau de Mestre em Ciências Biológicas.

Orientador: Prof. Dr. Celso Vataru Nakamura

Maringá
2018

Dados Internacionais de Catalogação-na-Publicação (CIP)
(Biblioteca Central - UEM, Maringá – PR, Brasil)

Z36i Zara, Raissa Benan
Investigação da atividade antitumoral de compostos heterocíclicos de nitrogênio em linhagem celular de câncer de próstata / Raissa Benan Zara. -- Maringá, PR, 2018.
30 f.: il. color.

Orientador: Prof. Dr. Celso Vataru Nakamura.
Dissertação (mestrado) - Universidade Estadual de Maringá, Centro de Ciências Biológicas, Programa de Pós-Graduação em Ciências Biológicas, 2018.

1. Câncer de próstata. 2. Atividade antitumoral. 3. Células PC3 - Câncer de próstata. 4. Mecanismo de ação. I. Nakamura, Celso Vataru, orient. II. Universidade Estadual de Maringá. Centro de Ciências Biológicas. Programa de Pós-Graduação em Ciências Biológicas. III. Título.

CDD 23.ed. 616.99463

Márcia Regina Paiva de Brito – CRB-9/1267

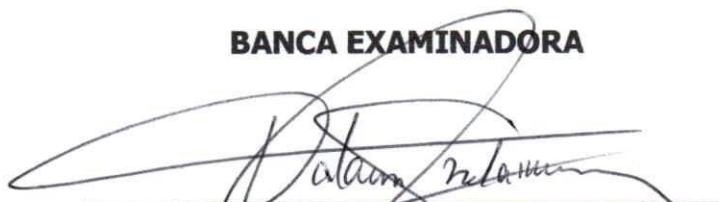
RAÍSSA BENAN ZARA

**INVESTIGAÇÃO DA ATIVIDADE ANTITUMORAL DE COMPOSTOS
HETEROCICLICOS DE NITROGÊNIO EM CÉLULAS DE CÂNCER DE
PRÓSTATA**

Dissertação apresentada ao Programa de Pós-Graduação em Ciências Biológicas (área de concentração - Biologia Celular e Molecular), da Universidade Estadual de Maringá para a obtenção do grau de Mestre em Ciências Biológicas.

Aprovado em: 20/09/2018

BANCA EXAMINADORA



Prof. Dr. Celso Vataru Nakamura
Universidade Estadual de Maringá



Profa. Dra. Elizandra Aparecida Britta Stefano
UniCesumar



Prof. Dr. Jean Henrique da Silva Rodrigues
Universidade Estadual de Maringá

BIOGRAFIA

Raíssa Benan Zara nasceu em Maringá, Paraná, no dia 15 de setembro de 1994. Possui graduação em Ciências Biológicas pela Universidade Estadual de Maringá (2012 – 2016). Em 2016 ingressou no mestrado do Programa de Pós-Graduação em Ciências Biológicas, área de concentração em Biologia Celular e Molecular, na mesma universidade, desenvolvendo seu trabalho no Laboratório de Inovação Tecnológica no Desenvolvimento de Fármacos e Cosméticos.

AGRADECIMENTOS

Agradeço primeiramente à Deus, por ter me guiado até aqui, porque se mostrou presente em todos os momentos e por todas as dificuldades que me fizeram crescer.

À minha família, que me apoiou em todos os momentos, por todo o incentivo e compreensão ao longo de minha vida.

Ao meu orientador, Prof. Dr. Celso Vataru Nakamura, pela oportunidade e por todo o auxílio, confiança e paciência durante esse período.

Aos colegas de laboratório, que de maneira geral, sempre me ajudaram nos momentos que precisei. Em especial, a Vanessa, a Karina, ao César e a Danielle.

Aos amigos, que indiretamente fizeram parte desse trabalho, com suas torcidas e orações, sempre dispostos a me ouvir quando tudo parecia dar errado ou compartilhar as alegrias quando tudo ia bem.

Ao Programa de Pós-Graduação em Ciências Biológicas, por essa oportunidade, principalmente aos professores, que contribuíram imensamente com a minha formação profissional.

À Coordenação de Aperfeiçoamento de Pessoal de Nível Superior (CAPES), pela concessão da bolsa de estudos.

Aos membros da banca examinadora, por terem aceitado o convite para contribuir com esse trabalho.

À todos, que direta ou indiretamente, contribuíram com esse trabalho, inclusive aos que eventualmente não foram citados.

Muito obrigada!!!

APRESENTAÇÃO

Em consonância com a resolução nº 038/2017 do Programa de Pós-Graduação em Ciências Biológicas da Universidade Estadual de Maringá, essa dissertação é composta por um resumo geral e um artigo científico, sendo este redigido de acordo com as normas da revista *Biology*, ISSN 2079-7737, Qualis CBI B1. O artigo, *Investigation of anticancer activity of quinoxalines and pirazines derivatives in cancer prostate cells*, envolve a caracterização da atividade antitumoral de uma série compostos heterocíclicos de nitrogênio em células de câncer de próstata, em especial, o 7-cloro-N-metil-3-(metilsulfonil)quinoxalin-2-amina, que mostrou melhor atividade na célula de interesse.

RESUMO GERAL

Introdução: Na América Latina e Caribe, o câncer de próstata é a principal causa de morte decorrente de câncer entre a população masculina. Entre os tratamentos convencionais estão a privação de andrógenos, prostatectomia, radioterapia e quimioterapia. No entanto, os tumores podem desenvolver resistência a castração e/ou sofrer metástases, o que torna estas intervenções limitadas e não-efetivas. Assim, é urgente a busca de novos compostos eficazes para estes pacientes. Nesse contexto, muitas substâncias têm sido testadas. Compostos com anéis heterocíclicos de nitrogênio, como as quinoxalinas e as pirazinas, destacam-se por apresentar um amplo espectro de atividade biológica, incluindo ação antitumoral. Além disso, as estruturas de pirazinas e quinoxalinas permitem variadas modificações, possibilitando a obtenção de uma ampla variedade de compostos com diferentes aplicações biológicas.

Objetivos: O objetivo desse trabalho foi avaliar a atividade antitumoral *in vitro* de dez compostos de quinoxalina e pirazina em cultura de células humanas de câncer de próstata andrógeno-independente (PC3) e sua toxicidade em células epiteliais normais de próstata (RWPE-1).

Os objetivos específicos foram analisar a viabilidade de células expostas aos derivados de quinoxalina e pirazina e identificar os compostos com atividade antitumoral; verificar alterações na morfologia sob microscopia ótica; observar o efeito na migração celular e verificar um possível estresse oxidativo que pode estar induzindo a morte celular.

Materiais e métodos: Oito compostos com núcleo de quinoxalina e dois com núcleo de pirazina foram sintetizados e fornecidos pelo Prof. Diego Pereira Sangi, da Universidade Federal Fluminense. A viabilidade celular foi determinada pelos ensaios do MTT, vermelho neutro e azul de tripano. Para os demais experimentos, as células foram tratadas com 7-cloro-N-metil-3-(metilsulfonyl)quinoxalin-2-amina com as concentrações de IC₁₀ e IC₅₀, 15.22 µM e 28.45 µM, respectivamente, com ou sem pré-incubação do antioxidante NAC. Foram observadas a morfologia e a migração das células, pelo ensaio de cicatrização de feridas, em microscópio invertido de contraste de fase. Foram mensurados a produção de H₂O₂, pela marcação com Amplex Red, e os níveis de tióis reduzidos, pelo DTNB. Em seguida, a detecção de peroxidação lipídica utilizou a marcação com DPPP. Ademais, foram realizadas microscopia de fluorescência, para visualização do potencial de membrana mitocondrial ($\Delta\Psi_m$) por TMRE, e foram mensurados os níveis de ATP intracelular pelo kit luminescente CellTiter-Glo. A integridade da membrana celular foi determinada por PI em espectrofluorímetro. Além disso, vesículas ácidas de células vivas foram marcadas com LysoTracker Red e visualizadas em microscopia de fluorescência.

Resultados e discussão: Apenas três dos dez compostos avaliados exibiram atividade em células PC3, sendo os compostos GSCB42, GSCB46, GSCB47 e, em menor intensidade, GSCB45, os quais são todos derivados de quinoxalina. Contudo, os compostos também apresentaram toxicidade em células RWPE-1. O padrão 2,3-substituintes em quinoxalina são conhecidos por proporcionar diferentes ambientes eletrônicos a molécula que influenciam na lipofilicidade e atividade dos compostos. O grupo metilsulfonyl na posição 3 é o principal substituinte que difere os compostos GSCB42 (7-chloro-N-methyl-3-(methylsulfonyl)quinoxalin-2-amine), GSCB46 (N-metil-3-(metilsulfonyl)quinoxalin-2-

amina), GSCB47 (3-cloro-6-metil-2-(metilsulfonil)quinoxalina) e GSCB45 (N,7-dimethyl-3-(methylsulfonyl)quinoxalin-2-amine) dos demais, portanto, são os principais responsáveis pela atividade destes compostos. Já o grupamento amina na posição 2 não parece ter alguma influência nessa característica.

O tratamento com o IC₁₀ e o IC₅₀ em células PC3 não causou alterações evidentes na morfologia, afetando apenas levemente o formato celular. No ensaio de cicatrização de feridas, GSCB42 não inibiu a proliferação das células para a área livre, o que sugere que o composto não exerce controle na inibição da metástase tumoral.

Estresse oxidativo é caracterizado por um desbalanço entre espécies reativas e o sistema antioxidante. O excesso de ROS pode induzir várias respostas biológicas, incluindo a iniciação de vias de transcrição de sinais, danos ou reparos no DNA entre outros, que desencadeiam apoptose, autofagia, necrose ou a sobrevivência celular. O tratamento com GSCB42 aumentou consideravelmente a produção H₂O₂ (267.7% no IC₅₀). No entanto, o composto não afetou os níveis de tios reduzidos. Uma das consequências do estresse oxidativo é a peroxidação lipídica, que aumentou em um efeito dose dependente nas células tratadas, atingindo 325,1% no IC₅₀. A pré-incubação com NAC foi capaz de reverter completamente o aumento nos níveis de ROS e a peroxidação lipídica.

A mitocôndria é um dos principais alvos dos elevados níveis de ROS, podendo exercer um papel central na apoptose. Para mensurar os danos mitocondriais, foram avaliados o potencial de membrana mitocondrial e os níveis intracelulares de ATP. GSCB42 parece afetar apenas os níveis de ATP, com uma pequena elevação no tratamento com o IC₅₀. Altos níveis da molécula podem ser encontrados durante a apoptose, podendo ser proveniente tanto da fosforilação oxidativa mitocondrial quanto de reações da glicólise.

Para avaliar se a morte decorre de necrose, foi determinado a integridade da membrana celular. Os resultados mostraram rompimento das membranas nos tratamentos com IC₁₀ e IC₅₀ de GSCB42. Possivelmente esse rompimento decorra da peroxidação lipídica ocasionada pelos níveis elevados de ROS. Já a autofagia, que é caracterizada por um acúmulo de autofagossomos e autolisossomos, foi verificada pela marcação de vesículas ácidas em células vivas pelo LysoTracker e visualização em microscópio de fluorescência. No entanto, não foram observadas diferenças na fluorescência de células controle ou tratadas.

Dessa forma, o tratamento com GSCB42 provocou elevação nos níveis de ROS, com a consequente peroxidação lipídica, que por sua vez, pode ter contribuído para o rompimento da membrana plasmática. Assim, os resultados sugerem que a morte celular das células tratadas com GSCB42 decorre de apoptose, possivelmente por meio de apoptose extrínseca visto que houveram poucas alterações mitocondriais. Além disso, ocorreu necrose nas linhagens PC3 tratadas com o composto GSCB42.

Conclusão: O “screening” possibilitou a identificação de quatro compostos com atividade antitumoral. O estresse oxidativo parece estar envolvido na morte celular e rompimento precoce da membrana. Estudos futuros são necessários para esclarecer a via de morte celular, assim como na modificação de novos compostos a partir destes, para potencializar a atividade antitumoral e aumentar a seletividade.

Palavras chaves: atividade antitumoral, câncer de próstata, células PC3, screening, compostos nitroheterocíclicos, mecanismo de ação.

GENERAL ABSTRACT

Introduction: In Latin America and Caribbean, prostate cancer is the leading cause of cancer death among men. Conventional treatments include androgen deprivation, prostatectomy, radiation therapy, and chemotherapy. However, tumors may develop resistance to castration and/or metastases, which makes these interventions limited and non-effective. Thus, the search for new compounds effective for these patients is urgently needed. In this context, many substances have been tested. Compounds with heterocyclic nitrogen rings, such as quinoxalines and pyrazines, detach as having a broad spectrum of biological activity, including antitumoral. In addition, pyrazine and quinoxaline structures allow for varied modifications, making it possible to obtain a wide variety of compounds with different biological applications.

Objectives: The objective of this study was to evaluate the *in vitro* antitumor activity of ten compounds of quinoxaline and pyrazine in culture of androgen-independent prostate cancer cells (PC3) and their toxicity in normal prostate epithelial cells (RWPE-1).

Specific objectives were to analyze the viability of cells exposed to quinoxaline and pyrazine derivatives and to identify compounds with antitumor activity; to verify changes morphology under optical microscopy; to observe the effect on cell migration and to verify a possible oxidative stress, which may be inducing cell death.

Materials and methods: Eight compounds with quinoxaline nucleus and two with pyrazine nucleus were synthesized and provided by Prof. Diego Pereira Sangi, from the Fluminense Federal University. Cell viability was determined by MTT, neutral red and trypan blue tests. For the remaining experiments, cells were treated with 7-chloro-N-methyl-3-(methylsulfonyl)quinoxalin-2-amine at concentrations of IC₁₀ and IC₅₀, 15.22 μ M and 28.45 μ M, respectively, with or without preincubation of NAC antioxidant. Morphology and cell migration were observed by the wound healing assay under inverted phase contrast microscopy. H₂O₂ production was measured using Amplex Red and reduced thiol levels by DTNB. Thereafter, detection of lipid peroxidation utilized DPPP marker. Moreover, fluorescence microscopy was performed to visualize the mitochondrial membrane potential ($\Delta\Psi_m$) by TMRE, and the intracellular ATP levels were measured by the CellTiter-Glo luminescent kit. Integrity of the cell membrane was determined by PI in a spectrofluorimeter. In addition, acidic vesicles from living cells were marked with LysoTracker Red and visualized under fluorescence microscopy.

Results and discussion: Only four of the ten evaluated compounds exhibited activity in PC3 cells, the compounds GSCB42, GSCB46, GSCB47 and, to a lesser extent, GSCB45, all derived from quinoxaline. However, the compounds also showed toxicity in RWPE-1 cells. The 2,3-substituent pattern in quinoxaline is known to provide different electronic environments to the molecule that influence the lipophilicity and activity of the compounds. The methylsulfonyl group at the 3-position is the major substituent that differs GSCB42 (7-chloro-N-methyl-3- (methylsulfonyl) quinoxalin-2-amine), GSCB46 (N-methyl-3- (methylsulfonyl) quinoxalin- 2-amine), GSCB47 (3-chloro-6-methyl-2-(methylsulfonyl) quinoxaline) and GSCB45 (N, 7-dimethyl-3- (methylsulfonyl) quinoxalin-2-amine) from others, therefore, are the main responsible for the activity of these compounds. The 2-position amine group does not seem to have any influence on this characteristic.

Treatment with IC₁₀ and IC₅₀ in PC3 cells did not cause obvious changes in morphology, only slightly affecting the cell format. In the wound healing assay, GSCB42 did not inhibit proliferation of the cells into the free area, which suggests that the compound exerts no control in inhibiting tumor metastasis.

Oxidative stress is characterized by an imbalance between reactive species and antioxidant system. Excess ROS can induce various biological responses, including initiation of signal transcription pathways, DNA damage or repairs among others, which trigger apoptosis, autophagy, necrosis, or cell survival. Treatment with GSCB42 considerably increased H₂O₂ production (267.7% on IC₅₀). However, compound did not affect reduced thiois levels. One of the consequences of oxidative stress is lipid peroxidation, which increased in a dose-dependent effect on treated cells, reaching 325.1% at IC₅₀. Preincubation with NAC was able to completely reverse the levels of ROS and lipid peroxidation.

Mitochondria are one of the main targets of high ROS levels and may play a central role in apoptosis. In order to measure mitochondrial damage, the mitochondrial membrane potential and intracellular ATP levels were evaluated. GSCB42 appears to affect only ATP levels, with a slight elevation in IC₅₀ treatment. High levels of the molecule can be found during apoptosis, and may be derived from both mitochondrial oxidative phosphorylation and glycolysis reactions.

To assess whether death results from necrosis, integrity of cell membrane was determined. The results showed rupture of the membranes in treatments with IC₁₀ and IC₅₀ of GSCB42. Possibly this disruption results from lipid peroxidation caused by elevated levels of ROS. Autophagy, which is characterized by an accumulation of autophagosomes and autolysosomes, was verified by marking acidic vesicles in living cells by LysoTracker and fluorescence microscopy. Nevertheless, no differences were observed in the fluorescence of control or treated cells.

Therefore, treatment with GSCB42 caused elevation in ROS levels, with consequent lipid peroxidation, which in turn may have contributed to the rupture of the plasma membrane. Thus, results suggest that the cell death of cells treated with GSCB42 occurs due from apoptosis, possibly through extrinsic apoptosis since there were few mitochondrial alterations. In addition, necrosis occurred in PC3 lines treated with compound GSCB42.

Conclusion: The screening allowed identification of four compounds with antitumor activity. Oxidative stress appears to be involved in cell death and early rupture of the membrane. Future studies are needed to clarify the cell death pathway, as well as modifying new compounds from these, to potentiate antitumor activity and increase selectivity.

Key words: antitumor activity, prostate cancer, PC3 cells, screening, nitroheterocyclic compounds, mechanism of action.

INVESTIGATION OF ANTICANCER ACTIVITY OF QUINOXALINE AND PYRAZINE DEVIVATIVES IN CANCER PROSTATE CELLS

Raíssa Benan Zara¹, Vanessa Kaplum², César Armando Contreras Lancheros³, Danielle Lazarin Bidoia³, Diego Pereira Sangi⁴, Celso Vataru Nakamura^{1,2,5}

¹Programa de Pós-Graduação em Ciências Biológicas, Universidade Estadual de Maringá

²Programa de Pós-Graduação em Ciências Farmacêuticas, Universidade Estadual de Maringá

³Complexo de Centrais de Apoio à Pesquisa (COMCAP), Universidade Estadual de Maringá

⁴Departamento de Química, Universidade Federal Fluminense

⁵Departamento de Ciências Básicas da Saúde, Universidade Estadual de Maringá

Abstract

Prostate cancer is the most common cancer in Latin America and the Caribbean. Metastatic and androgen deprivation resistant tumors do not have a good prognosis, making the development of new effective treatments crucial. In this work, a screening of ten N-containing heterocyclic compounds was performed on PC3 and RWPE-1 cells. Cell viability was determined by MTT, neutral red and trypan blue assays. Four compounds showed antitumor activity, 7-chloro-N-methyl-3-(methylsulfonyl)quinoxalin-2-amine (GSCB42), N-methyl-3-(methylsulfonyl)quinoxalin-2-amine (GSCB46), 3-chloro-6-methyl-2-(methylsulfonyl)quinoxaline (GSCB47) and, in a lower intensity, N,7-dimethyl-3-(methylsulfonyl)quinoxalin-2-amine (GSCB45). The activity of these compounds appears to be mainly related to the 3-position methylsulfonyl group. However, none of the compounds exhibited selectivity compared to non-tumor cells. In addition, possible effects of 7-chloro-N-methyl-3-(methylsulfonyl)quinoxalin-2-amine on morphology, cell migration, oxidative stress, mitochondrial membrane potential and formation of autophagic vesicles were evaluated. GSCB42 was not able to inhibit cell migration. On the other hand, the compound caused H₂O₂ increase, lipid peroxidation and loss of cell membrane integrity. The results suggest that the pathway of extrinsic apoptosis and necrosis are involved in cell death of tumor cells.

Keywords: nitroheterocycles compounds, screening, anticancer activity, PC3 cells, RWPE-1 cells, mechanism of action.

1. Introduction

Cancer is the second leading cause of death around the world, accounting for about 1 in 6 deaths [1]. In Latin America and the Caribbean, prostate cancer has the highest incidence rate in men and is the leading cause of cancer-related death in population [2]. Factors such as age, race, and family history of prostate cancer have been closely related to disease lethality [3].

Conventional treatments against the prostate cancer involve, alone or in combination, androgenic ablation therapy, prostatectomy, radiotherapy, cytotoxic chemotherapy [4]. These therapies have a high cure rate in localized tumor patients, however there is no efficient treatment for metastatic cancer [5]. Furthermore, several tumors acquire resistance to castration during treatment with androgen deprivation. Therapies then become limited and non-effective, resulting in the death of the patient.

In this context, treatment with docetaxel associated with prednisone was the first chemotherapeutic that showed an increase in overall survival, although its use is limited by age and preexisting diseases. Other medicines, such as cabazitaxel, abiraterone acetate, enzalutamide, sipuleucel T, radium-223, and denosumab, were approved in the last decade. However, metastatic prostate cancer resistant to castration remains incurable [6].

Quinoxalines and pyrazines are an important class of nitrogen containing heterocyclic compounds that is known for its broad spectrum of biological activities, including antimicrobial [7-13], antiproliferative [14-16], anti-inflammatory [17] antidepressant and anxiolytic [18], antihyperglycemic [19], and antitumoral [20-23].

Based on that, we performed a screening of a series of nitrogen containing heterocyclic compounds in castration-resistant prostate cancer cells (PC3) and epithelial prostate cells (RWPE-1). Then, we investigated possible effects in cell migration and oxidative stress in cells treated with a quinoxaline derivative, 7-chloro-N-methyl-3-(methylsulfonyl)quinoxalin-2-amine (GSCB42).

2. Material and Methods

2.1 Chemicals

Dimethyl sulfoxide (DMSO), digitonin, diphenyl-1-pyrenylphosphine (DPPP), *N*-acetylcysteine (NAC), tetramethylrhodamine ethyl ester (TMRE) and 5,5-dithio-bis-2-nitrobenzoic acid (DTNB) were purchased from Sigma Chemical Co. (St. Louis, MO, USA). Amplex Red Hydrogen Peroxidase/Peroxidase Assay Kit, LysoTracker Red DND-99, propidium iodide (PI) and 3-(4,5-dimethyl-thiazol-2-yl)-2,5-diphenyltetrazolium bromide (MTT) were obtained from Invitrogen (Eugene, OR, USA). Fetal bovine serum (FBS), Keratinocyte-SFM (K-SFM) medium and Roswell Park Memorial Institute (RPMI 1640) medium were purchased from Invitrogen (Grand Island, NY, USA). Cell Titer-Glo Luminescent Cell Viability Assay was purchased from Promega (Madison, WI, USA). Trypan Blue was obtained from Acros Organics (Fair Lawn, NJ, USA). Neutral red was

obtained from Alamar Tecno-Científica (Diadema, SP, Brazil). All of the others reagents were of analytical grade.

2.2 Synthesis of compounds

A library of nitrogen containing heterocyclic compounds, with quinoxaline or pyrazine core (Fig.1), were provided by Professor Diego Pereira Sangi, from the Institute of Exact Sciences of the Chemistry Department of the Fluminense Federal University. Stock solutions were prepared aseptically in DMSO and diluted in culture medium so that DMSO concentration did not exceed 1% in the experiments.

2.3 Cells

Prostate adenocarcinoma cells (PC3) were maintained in RPMI 1640 medium supplemented with FBS, while prostate epithelial cells (RWPE-1) were cultured in K-SFM medium with recombinant human epidermal growth factor (rhEGF) and bovine pituitary extract (BPE). Both cells were grown in moist atmosphere with 5% CO₂ at 37 °C.

2.4 Cell viability

Cell viability was determined by MTT, neutral red uptake and trypan blue assay. PC3 and RWPE-1 cells were seeded at a density of 2.5 x 10⁵ cells mL⁻¹ and 4.0 x 10⁵ cells mL⁻¹, respectively, in 96-well plates for MTT and neutral red assays and 24 wells plates for the trypan blue test. Cells were incubated for 24 h at 37 °C under a 5% CO₂ atmosphere. Then, cells were treated with compounds at different concentrations (1, 10, 50 and 100 μM) for 48 h.

For MTT assay, the medium was replaced by MTT (50 μL; 2 mg.mL⁻¹) and plate was incubated in the dark at 37 °C for 4 h. Then, medium was removed, the resulting formazan crystals were dissolved in DMSO, and absorbance read at 570 nm in a microplate reader (BioTek Power Wave XS spectrophotometer).

For red neutral uptake assay, medium was replaced with neutral red dye (40 μg mL⁻¹) in medium for 3 h. The cells were then washed in 1% CaCl₂ and 2% formaldehyde and dye retained by viable cells was extracted by addition of a 30% solution of acetic acid in ethanol/water (50%). Absorbance was determined at 540 nm in a microplate reader (BioTek Power Wave XS spectrophotometer).

For trypan blue exclusion staining, medium was aspirated after treatment and cells were detached by trypsinization, collected and centrifuged at 10,000 rpm for 10 min. Cells were then resuspended in PBS and added 0.4% trypan blue (1:1). Count of viable cells and dead cells were performed under an optical microscope (Olympus CX31).

Percentage of viable cells was determined in comparison to the control. IC₁₀ and IC₅₀ values were determined by non-linear regression analysis as the concentration required to reduce absorbance or percentage of viable cells at 50% compared to the control cells.

2.5 Morphology of prostate cancer cells

PC3 cells were seeded at a density of $2.5 \text{ cells mL}^{-1}$ for 24 h at 37°C under a 5% CO_2 atmosphere. After that, cells were preincubated with or without NAC (5 mM) for 2 h and treated with 7-chloro-N-methyl-3-(methylsulfonyl)quinoxalin-2-amine (GSCB42) ($15.22 \mu\text{M}$ and $28.45 \mu\text{M}$, IC_{10} and IC_{50} , respectively) for 48 h. All experiments below were performed with same cell preparation. Cell morphology was observed under inverted phase contrast microscope (40x; Olympus CKX41). Images were captured with a Olympus SC30 camera.

2.6 Wound healing migration assay

Wound healing assay was evaluated according Liang et al [24]. PC3 cells were grown in 24-well plate. Then they were incubated with 0.5% FBS for 6 h. Cells were scratched with a $200 \mu\text{L}$ tip and washed with PBS prior to treatment of the cells with GSCB42 (IC_{10} and IC_{50}) for 24 and 48 h. Cell migration was recorded using an inverted phase contrast microscope (5x; Olympus CKX41). Images were captured with a Olympus SC30 camera and area of the wound was calculated using Image J software.

2.7 Measurement of H_2O_2

Production of H_2O_2 was evaluated using Amplex RED. Hydrogen peroxide (H_2O_2 ; $200 \mu\text{M}$) was used as a positive control. PC3 cells treated with GSCB42 (IC_{10} and IC_{50}) for 48 h were detached by trypsinization, resuspended in PBS and marked with $12 \mu\text{M}$ Amplex RED and 0.05 IU mL^{-1} horseradish peroxidase. Fluorescence intensity was measured in a fluorescence microtiter reader (VICTOR X3, PerkinElmer) with excitation and emission wavelength of 530 and 590 nm, respectively. Fluorescence was normalized by number of cells [25].

2.8 Measurement of reduced thiol levels

Reduced thiols levels were evaluated using DTNB (5,5-dithio-bis-2-nitrobenzoic acid). PC3 cells were plated and treated with GSCB42 (IC_{10} and IC_{50}) as described above. Hydrogen peroxide (H_2O_2 ; $200 \mu\text{M}$) was used as a positive control. Medium was removed and replaced by Tris-HCl buffer (10 mM, pH 2.5), followed by sonication (Branson Ultrasonics SLPe Digital Sonifier Cell Disruptor) in icy water for 1 min with vortexing every two seconds. Non-soluble portions were removed by centrifugation. Then, $100 \mu\text{L}$ of supernatant, $100 \mu\text{L}$ of phosphate buffer (500 mM, pH 7.5) and $20 \mu\text{L}$ of DTNB (1 mM). Absorbance was measured in a microplate reader (BioTek PowerWave XS spectrophotometer) at 412 nm.

2.9 Cell membrane integrity

Cell membrane integrity was evaluated using PI. Digitonin ($80 \mu\text{M}$) was used as a positive control. PC3 cells treated with GSCB42 (IC_{10} and IC_{50}) were detached by trypsinization, resuspended in PBS and marked with PI ($4 \mu\text{g mL}^{-1}$) for 5 min at room temperature. Fluorescence was measured in a fluorescence microtiter plate reader

(VICTOR X3, PerkinElmer) with excitation and emission wavelength of 480 and 580 nm, respectively. Fluorescence was normalized by number of cells [25].

2.10 Lipid peroxidation

Lipid peroxidation was evaluated using DPPP. Hydrogen peroxide (H_2O_2 ; 200 μM) was used as a positive control. PC3 cells treated with GSCB42 (IC_{10} and IC_{50}) were detached by trypsinization, resuspended in PBS and marked with 50 μM DPPP for 15 min at room temperature. Fluorescence was measured in a fluorescence microplate reader (VICTOR X3, PerkinElmer) with excitation and emission wavelength of 351 and 460 nm, respectively. Fluorescence was normalized by number of cells [25].

2.11 Determination of intracellular ATP

Intracellular ATP was evaluated using the CellTiter-Glo reagent. KCN (1000 μM) was used as a positive control. PC3 cells treated with GSCB42 (IC_{10} and IC_{50}) were detached by trypsinization, resuspended in PBS and marked with CellTiter-Glo reagent for 10 min at room temperature. Luminescence intensity was measured in a fluorescence microtiter reader (VICTOR X3, PerkinElmer). Luminescence was normalized by number of cells [25].

2.12 Determination of mitochondrial membrane potential

Mitochondrial membrane potential ($\Delta\Psi_m$) was evaluated using TMRE. PC3 cells treated with GSCB42 (IC_{10} and IC_{50}) were marked with TMRE (25 nM) for 30 min at 37°C. Fluorescence was observed in a fluorescence microscope (Olympus BX51), and the images were captured with an Olympus UC30 camera.

2.13 Visualization of acidic vesicles in living cells

Acidic vesicles were evaluated using LysoTracker. PC3 cells treated with GSCB42 (IC_{10} and IC_{50}) were marked with LysoTracker Red DND99 (50 nM) for 15 min at 37 °C. Fluorescence was observed in a fluorescence microscope (Olympus BX51), and the images were captured with an Olympus UC30 camera.

2.14 Statistical Analysis

Data were expressed as mean \pm standard deviation (SD) of independent experiments. Statistical analysis was performed using GraphPad Prism® 6.0 software (CA, USA). Data were analyzed using one-way or two-way analysis of variance (ANOVA) and values of $p < 0.05$ were considered statistically significant.

3. Results and Discussion

Since prostate cancer is one of the most lethal neoplasias in men and considering resistance to major treatments, androgen deprivation and docetaxel, it becomes necessary

and urgent to identify new potential treatments for prostate cancer. Chemotherapy has been prominent, with great efforts aimed at the design and development of new drugs with antitumor activity [26].

Several compounds, with nitrogen containing heterocyclic core, have been tested in the treatment of neoplasias, exhibiting different mechanisms of action. Compound 1-Allyl-3-(2-(4-(dimethylamino)benzylidene)hydrazinyl)-quinoxalin-2(1H)-one, for example, demonstrated a potent activity in liver (HepG2) and breast (MCF-7) cancer cells lines, acting as an inhibitor of the c-kit enzyme, a member of the protein tyrosine kinase III family [27]. BMS-345541 [4-(2'-aminoethyl)amino-1,8-dimethylimidazo(1,2-a)quinoxaline]-4,5-dihydro-1,8-dimethyl-midazo(1,2 α)quinoxalin-4-one-2-carboxylic acid also showed good results in melanoma cells and melanoma tumors *in vivo*, targeting the NK- κ B pathway IKK protein which regulates expression of antiapoptotic proteins [28]. In addition, some quinoxalines may act as hypoxia-selective, such as the inhibitor of HIF-1 α 6-Chloro-2-(4-chloro-phenyl)-quinoxaline-1,4-di-N-oxide [29].

In this context, quinoxaline nuclei are known to exhibit antitumor activity [30]. The electronic and physicochemical properties of the heterocyclic compounds provide a key in the optimization of drug candidates, functioning as a precursor for a large number of compounds [31,32].

In the present work, eight compounds quinoxalines-derivatives and two compounds pyrazines-derivatives (Fig. 1) previously synthesized were evaluated for their antiproliferative activity in PC3 and RWPE-1 cells. To assess this, cells were treated at different concentrations for 48 h and analyzed by MTT, trypan blue and neutral red assays (Table 1). MTT is a tetrazolium salt that is converted into formazan crystals by the succinate dehydrogenase into the mitochondria. Because it is impermeable to cell membranes, the formazan accumulates in healthy cells. Neutral red uptake assay is based on the accumulation of the dye by lysosomes. In addition, trypan blue exclusion test follows the principle that living cells have intact membranes impermeable to dye, while non-viable cells will have a blue cytoplasm. It has previously been shown that different assays may present different results depending on the agent and assay used [33-35].

Among the ten compounds tested, GSCB42, GSCB46 and GSCB47 showed antitumor activity in prostate cancer cells and GSCB45 had moderate activity. However, these compounds did not show selectivity to the tumor cells. In addition, compounds containing pyrazine nucleus, GSCB50 and GSCB51, did not exhibit antitumor activity.

The 2,3-disubstituted quinoxaline standard is commonly studied by providing different electronic environments to the molecule, which may affect lipid profile and increase activity in target molecules [36]. By analyzing the structure and activity of the evaluated compounds, the major substituent responsible for conferring antitumor activity to the compounds is the 3-position methylsulfonyl group. Despite using a different biological model, Cogo [14] showed that this same group in similar compounds confers antiproliferative activity on *Leishmania amazonensis* and *Trypanosoma cruzi*. In addition, the results suggest that the 2-position amine grouping does not affect the activity of the compounds.

Substitution at the 7-position by a chlorine atom apparently increase cytotoxicity against RWPE-1 cells, although this reduction was not accompanied by less cytotoxicity against PC3 cells (GSCB41 vs GSCB43 and GSCB42 vs GSCB46). Reduction in cell viability caused by a chlorine atom in 6- and 7-positions in a quinoxaline ring were also observed by Ghanbarimasir [26] in breast and colon cancer cell lines.

Furthermore, by comparing compounds GSCB45, GSCB46 and GSCB47, the 7-position methyl substituent appears to reduce the action of the compounds, whereas the 2-position chlorine atom seems to improve activity.

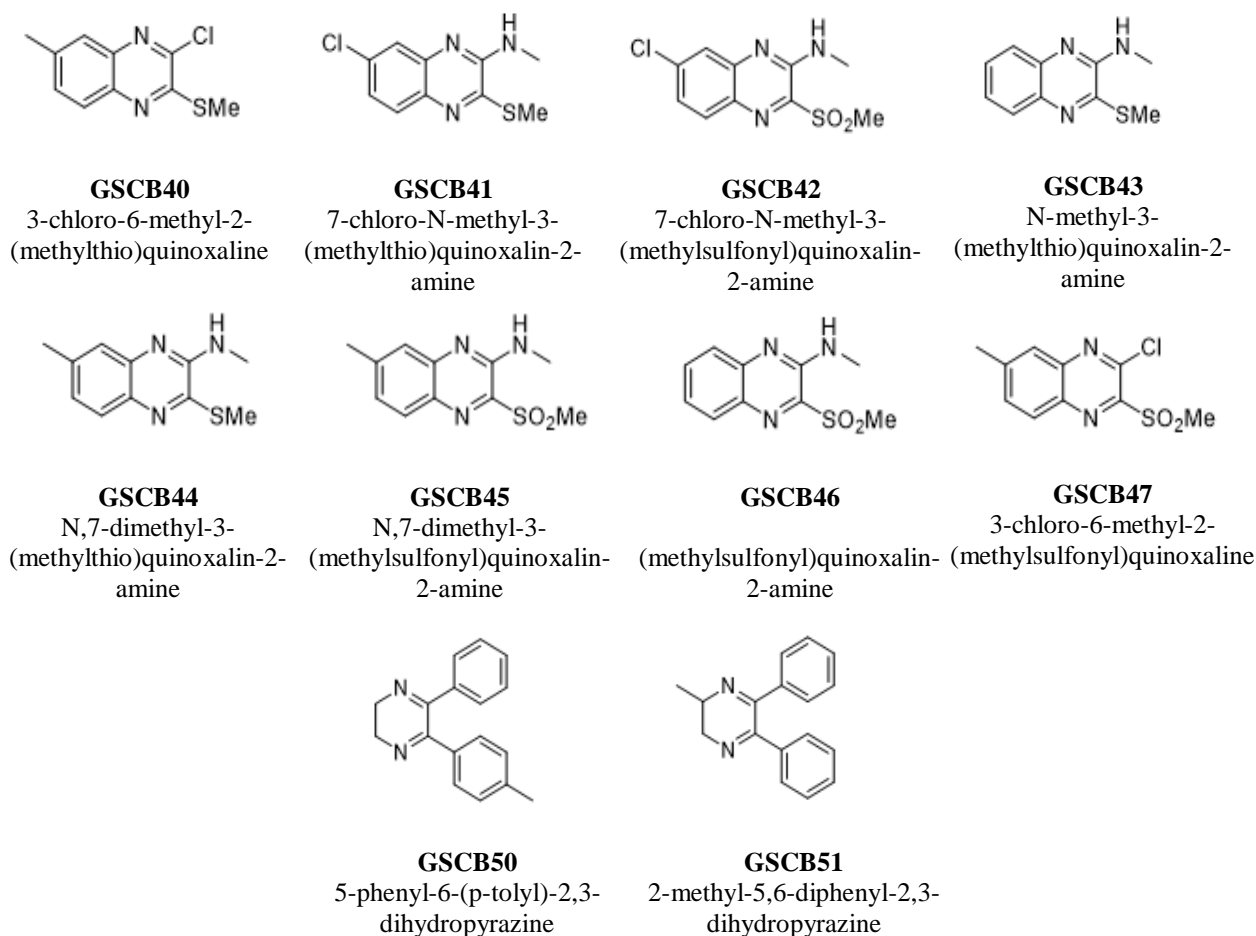


Figure 01. Chemical structure of the quinoxaline and pyrazine derivatives evaluated.

Table 01. Cell viability of different heterocyclic nitrogen compounds in prostate cancer cells (PC3) and prostate epithelial cells (RWPE-1)

| Compounds | PC3 (μM) | | | RWPE-1 (μM) | | |
|---|-----------------------|-------------------|-------------------|--------------------------|------------------|------------------|
| | MTT | Neutral Red | Trypan Blue | MTT | Neutral Red | Trypan Blue |
| GSCB40 (3-chloro-6-methyl-2-(methylthio)quinoxaline) | >100 | >100 | >100 | 76.74 \pm 8.49 | >100 | >100 |
| GSCB41 (7-chloro-N-methyl-3-(methylthio)quinoxalin-2-amine) | >100 | >100 | >100 | 99.59 \pm 22.28 | >100 | >100 |
| GSCB42 (7-chloro-N-methyl-3-(methylsulfonyl)quinoxalin-2-amine) | 28.45 \pm 1.17 | 7.61 \pm 0.54 | 27.55 \pm 3.50 | 6.22 \pm 0.99 | 7.61 \pm 1.33 | 5.61 \pm 0.66 |
| GSCB43 (N-methyl-3-(methylthio)quinoxalin-2-amine) | >100 | >100 | >100 | >100 | >100 | >100 |
| GSCB44 (N,7-dimethyl-3-(methylthio)quinoxalin-2-amine) | >100 | >100 | >100 | >100 | >100 | >100 |
| GSCB45 (N,7-dimethyl-3-(methylsulfonyl)quinoxalin-2-amine) | 85.56 \pm 3.50 | 92.80 \pm 15.41 | 85.38 \pm 16.85 | 57.79 \pm 9.95 | 36.69 \pm 2.74 | 80.19 \pm 2.31 |
| GSCB46 (N-methyl-3-(methylsulfonyl)quinoxalin-2-amine) | 28.54 \pm 1.02 | 24.99 \pm 2.01 | 26.15 \pm 0.93 | 30.31 \pm 8.66 | 27.03 \pm 3.08 | 27.21 \pm 2.40 |
| GSCB47 (3-chloro-6-methyl-2-(methylsulfonyl)quinoxaline) | 34.14 \pm 6.28 | 8.85 \pm 0.98 | 31.36 \pm 9.22 | 41.40 \pm 9.84 | 7.05 \pm 0.93 | 20.31 \pm 3.14 |
| GSCB50 (5-phenyl-6-(p-tolyl)-2,3-dihydropyrazine) | >100 | >100 | >100 | 85.90 \pm 6.42 | >100 | >100 |
| GSCB51 (2-methyl-5,6-diphenyl-2,3-dihydropyrazine) | >100 | >100 | >100 | >100 | >100 | >100 |

Results are presented as $\text{IC}_{50} \pm$ standard deviation.

In order to evaluate the possible changes and cell death induced by the treatment, we chose the compound GSCB42 to proceed with the experiments. Although the neutral red assay was more sensitive in these cells, concentrations of IC_{10} and IC_{50} were defined using the MTT method (15.22 μM and 28.45 μM respectively), since it is the most widely used currently.

Morphology of cells treated with GSCB42 was observed under optical phase contrast microscopy (Fig. 2). Cells treated with IC_{50} showed only a slight change in cell format, acquiring a rounded appearance, which was not observed in cells preincubated with NAC.

Wound-healing assay is a simple and unexpensive method that mimics migration of cells *in vivo*. In this assay, a scratch is created on a confluent cell monolayer opening a cell-free area that induces the cells to migrate into the gap. This migration occurs in diverse processes including cancer metastasis [37, 38]. Migration of prostate cancer cells was observed after 24 h and 48 h treatment with GSCB42 (Fig 3). After 48 h cultivation, wounds were practically closed, both control and treatment with IC_{10} and IC_{50} . Therefore,

7-chloro-N-methyl-3-(methylsulfonyl)quinoxalin-2-amine did not inhibit cell migration and then has no potential for inhibition of metastasis.

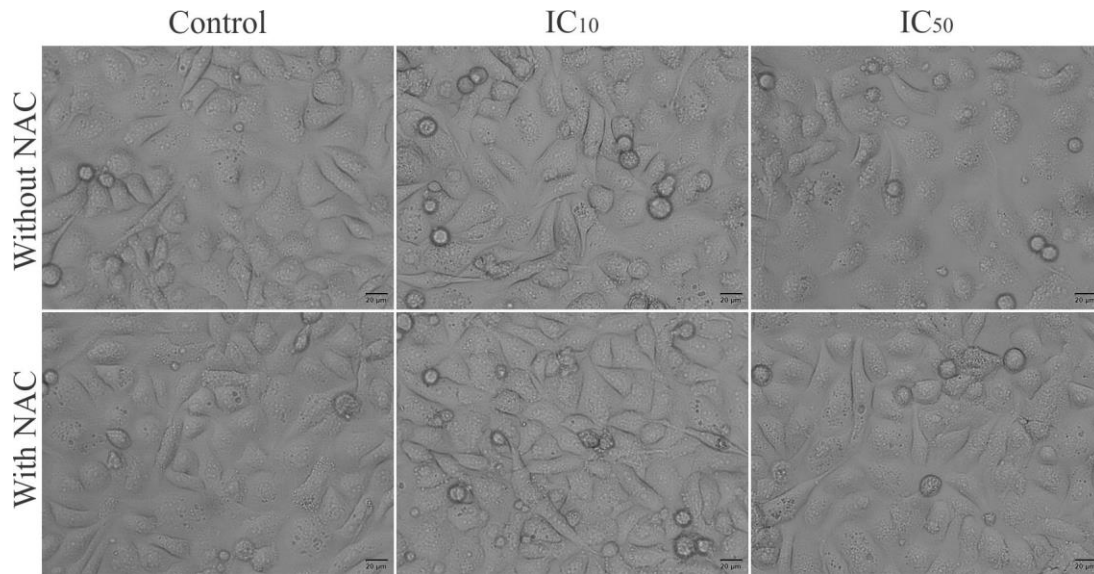


Figure 2. Effects of GSCB42 (IC₁₀ and IC₅₀) for 48 h on cell morphology of prostate cancer cells (PC3) with or without pre-incubation with NAC (5 mM) for 2 h. The bar is equivalent to 20 μm.

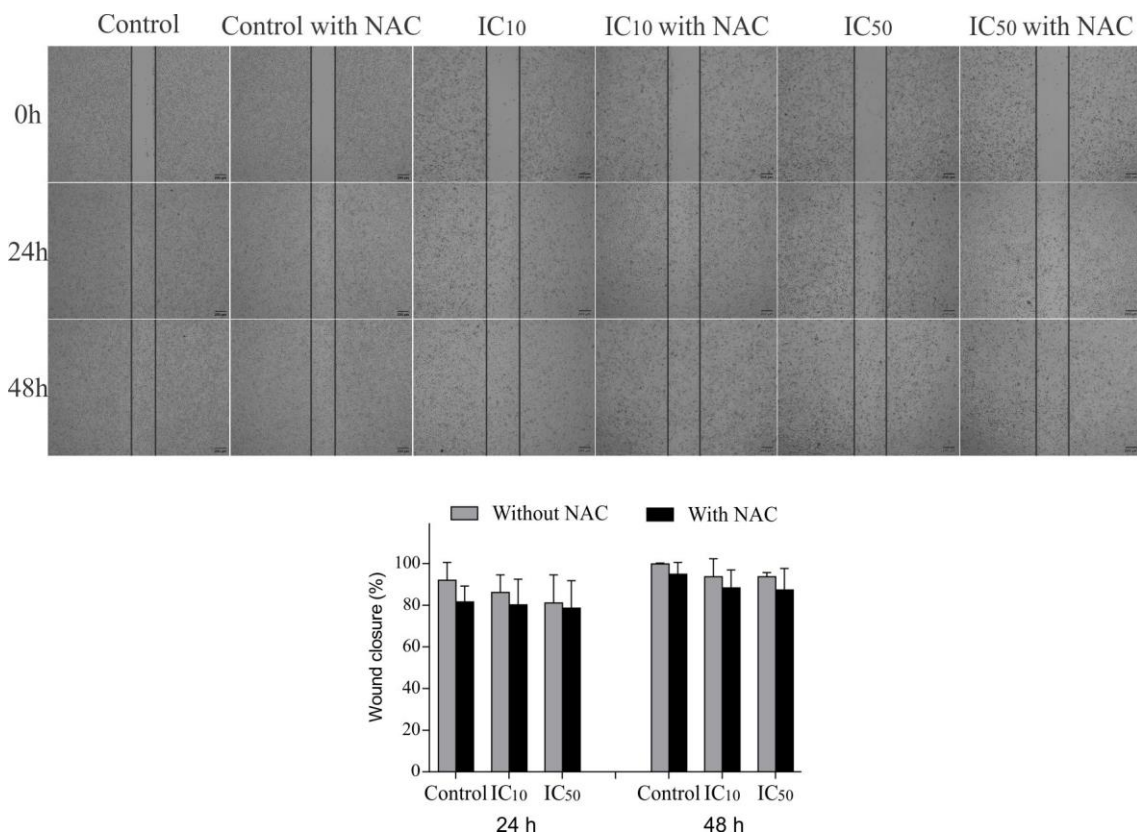


Figure 3. Effects of GSCB42 (IC₁₀ and IC₅₀) on cell migration by wound healing assay. PC3 cells were treated for 24 h and 48 h, with or without pre-incubation with NAC (5

mM) for 2 h. The data are expressed as percentage of wound closure \pm SD of three independent experiments. The bar is equivalent to 200 μ m.

Several tumor cell lines are characterized by high levels of reactive oxygen species (ROS), including prostate neoplasia. Factors such as proliferation, promotion of genetic mutations and instability, sensitivities to anticancer agents, invasion, and metastasis are all involved with this inherent oxidative stress. On the other hand, excessive ROS levels can trigger pro-apoptotic pathways and induce cell death in cancer models [3, 39].

To evaluate if oxidative stress was occurring in cells exposed to GSCB42, measurements of H₂O₂ production, reduced thiol levels and lipid peroxidation were performed. As one of the most stable ROS, H₂O₂ is commonly used to accompany ROS reduction products [40,41]. The production of H₂O₂ was determined using Amplex Red that reacts with H₂O₂ in a horseradish peroxidase (HRP) catalyzed reaction producing resofurin, a highly fluorescent compound [42]. PC3 cells showed a significant increase in H₂O₂ levels of 184.9 and 267.7%, after treatment with IC₁₀ and IC₅₀ of GSCB42 (Fig. 4a), respectively. Incubation with NAC was able to completely reverse this effect.

An indicator of oxidative stress is glutathione (GSH) level. Reactive oxygen species, such as H₂O₂, in addition to xenobiotics and other organic radicals, are neutralized by GSH, which is oxidized to form glutathione disulfide (GSSG). On the other hand, GSSG is recycled to GSH by a cascade of reactions involving glutathione peroxidase (GPx), glutathione-S-transferases (GST) and glutathione reductase (GR). Thus, under oxidative stress can be observed unbalance in the GSH / GSSG ratio [43, 44]. Reduced thiols levels were measured using DTNB, a reagent that oxidizes glutathione (GSH) to yield a yellow compound 5'-thio-2-nitrobenzoic acid (TNB). Although it caused an increase in H₂O₂ production, treatment of PC3 cells with GSCB42 showed only a slight reduction in the reduced thiols levels in cells treated IC₅₀ (Fig. 4b).

Lipid peroxidation is one of the main consequences of oxidative stress. Free radicals oxidize unsaturated fatty acids, with a reaction spreading a large number of substrates [45]. Lipid peroxidation was determined using the DPPP marker, that reacts with hydroperoxides to produce diphenyl-1-pyrenylphosphine oxide (DPPP = O), a fluorescent compound [46]. An increase of the 325.1% in lipid peroxidation was observed in PC3 cells treated with the compound at IC₅₀. The antioxidant NAC completely reversed this effect (Fig. 4c).

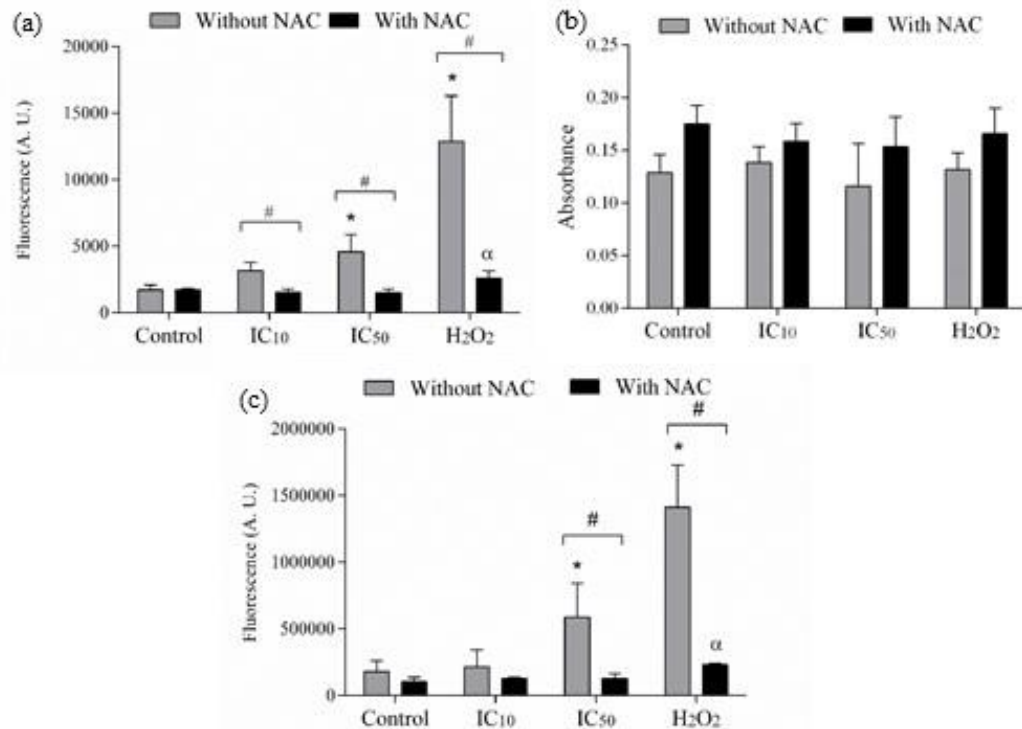


Figure 4. Effects of GSCB42 (IC₁₀ and IC₅₀) on oxidant system in prostate cancer cells (PC3). (a) H₂O₂ levels measurement was conducted using the Amplex Red kit. (b) Reduced thiois levels were measured using DTNB assay. (c) Lipid peroxidation was determined using DPPP marker. Cells were treated for 48 h, with or without pre-incubation with NAC (5 mM) for 2 h. H₂O₂ was used as a positive control. Results are expressed as mean \pm SD of at least three independent experiments. * $p \leq 0.05$, significant difference from control (untreated cells; one-way ANOVA followed by Dunnett's post hoc test); $\alpha p \leq 0.05$, significant difference from control + NAC (one-way ANOVA followed by Dunnett's post hoc test); # $p \leq 0.05$, significant difference between treatment with and without NAC (two-way ANOVA followed by Tukey post hoc test).

Mitochondria are important targets of high levels of ROS, so it plays a central role in apoptosis [47]. Mitochondrial apoptotic control involves maintenance of ATP production, maintenance of $\Delta\Psi_m$, and mitochondrial membrane permeability [48]. In order to evaluate if mitochondrial damage participate in the cell death pathway, $\Delta\Psi_m$, and intracellular levels of ATP were analyzed.

The $\Delta\Psi_m$ was observed in fluorescence microscopy using TMRE labeling, a lipophilic cation that accumulates in the mitochondrial matrix. Membrane depolarization implies less marker retention [49]. Control cells marked with TMRE exhibited intense cytoplasmic labeling. No change in fluorescence intensity was observed in cells treated with GSCB42 and cells incubated with NAC (Fig. 5a).

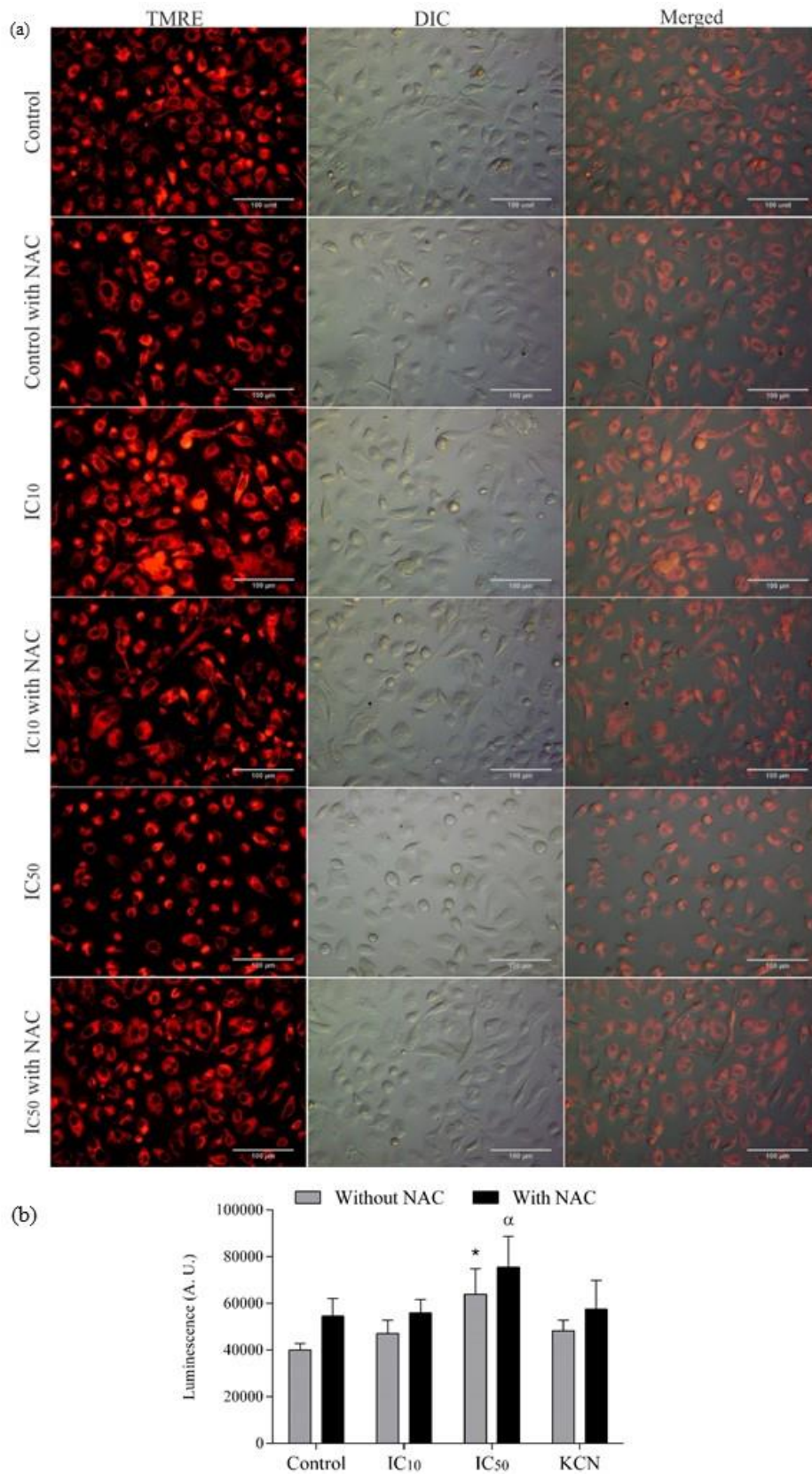


Figure 5. Effects of GSCB42 (IC₁₀ and IC₅₀) on mitochondrial membrane potential and ATP levels in prostate cancer cells (PC3). (a) Fluorescence microscopy analysis using

TMRE. (b) Intracellular ATP levels were measured using CellTiter Glo Kit. KCN was used as a positive control. Prostate cancer cells were treated for 48 h, with or without pre-incubation with NAC (5 mM) for 2 h. Results are expressed as mean \pm SD of three independent experiments. * $p \leq 0.05$, significant difference from control (untreated cells; one-way ANOVA followed by Dunnett's post hoc test); ^a $p \leq 0.05$, significant difference from control + NAC (one-way ANOVA followed by Dunnett's post hoc test). The bar is equivalent to 100 μ m.

Intracellular ATP levels were measured by CellTiter-Glo luminescent cell viability assay. This kit uses the luciferase reaction, which requires ATP to produce oxyluciferin and releasing luminescence proportional to the amount of ATP present [50]. GSCB42-treated PC3 cells with IC₅₀ showed an increase of 159.5% in ATP levels (Fig. 5b). Cells pre-incubated with NAC followed this increment.

To verify whether necrosis plays a role in GSCB42-induced cell death, cell membrane integrity was determined by marking with PI, a membrane impermeable fluorescent dye. When there are lesions on the membrane, PI is able to enter the cell and intercalate with DNA, blushing the nucleus [51]. The results showed an increase of 164.5% and 212.5% in PI fluorescence in cells treated with IC₁₀ and IC₅₀, respectively (Fig. 6). Loss of membrane integrity can occur due to peroxidation of membrane lipids, which compromises their function [52]. Pre-incubation with NAC antioxidant was able to reverse this effect.

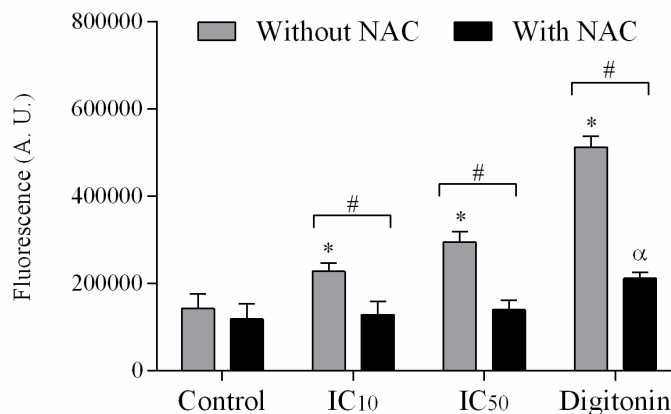


Figure 6. Effects of GSCB42 (IC₁₀ and IC₅₀) on cell membrane integrity in prostate cancer cells (PC3). Cells were treated and 48 h, with or without pre-incubation with NAC (5 mM) for 2 h. Integrity of the cell membrane was determined by fluorescent dye PI. Digitonin was used as a positive control. Results are expressed as mean \pm SD of three independent experiments. * $p \leq 0.05$, significant difference from control (untreated cells; one-way ANOVA followed by Dunnett's post hoc test); ^a $p \leq 0.05$, significant difference from control + NAC (one-way ANOVA followed by Dunnett's post hoc test); # $p \leq 0.05$, significant difference between treatment with and without NAC (two-way ANOVA followed by Tukey post hoc test).

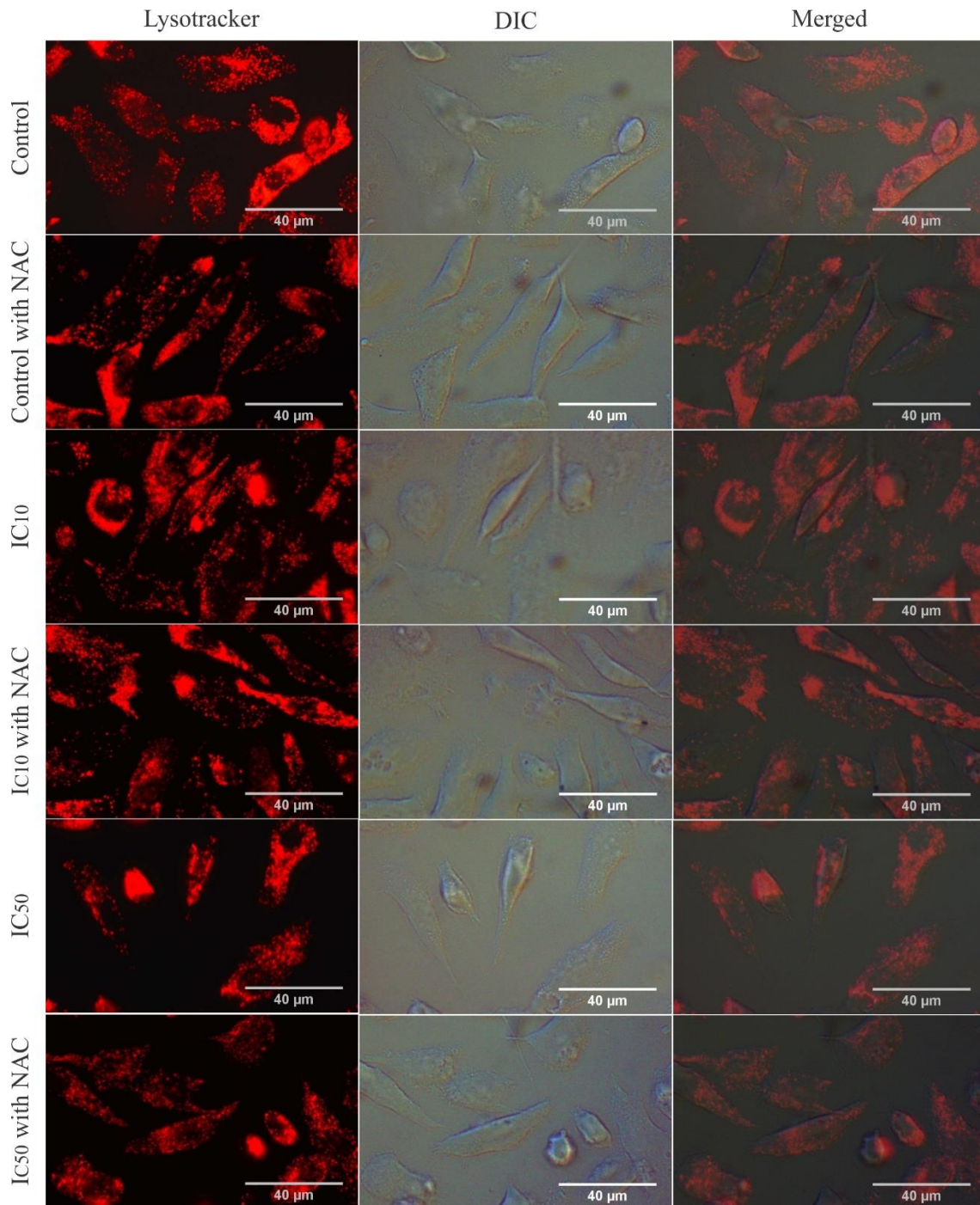


Figure 7. Fluorescence microscopy analysis of prostate cancer cells (PC3) using the marker Lysotracker Red. PC3 cells were treated with GSCB42 (IC₁₀ and IC₅₀) for 48 h with or without pre-incubation with NAC (5 mM) for 2 h. The bar is equivalent to 40 μ m.

The principal evidence of cellular autophagy is an intense vacuolization of the cytoplasm, with accumulation of autophagosomes and autolysosomes. To assess the participation of the autophagy pathway in the toxicity of GSCB42, acid vesicles were observed under fluorescence microscopy using LysoTracker Red. This marker is constituted by a fluorophore linked to a weak base that is protonated in neutral pH. Upon protonation, the molecule is retained in the acidic organelle [53]. Control and treated cells

were marked with LysoTracker Red and exhibited a bright fluorescence, with no significant differences between them (Fig. 7). As there was no increase in the labeling of acidic vesicles, cell death due to autophagy is probably not occurring.

Oxidative stress is characterized by imbalance between reactive species and antioxidant defense mechanism. GSCB42 caused a large increase in H₂O₂ production, one of the main forms of ROS. Although the increase of hydrogen peroxide has discreetly altered the GSH/GSSG ratio, this does not eliminate the probability of an imbalance in the antioxidant system, since the enzymes act in a compensatory way. Increased oxidative stress can induce various biological responses, including adaptation, cell cycle arrest, gene transcription, initiation of signal transcription pathways, DNA repair or damage, among others, which will determine whether the cell will undergo apoptosis, necrosis, autophagy or survive [54].

The drastic reduction of cell membrane integrity associated with high levels of ROS may suggest that GSCB42 triggers a necrotic process in treated cells. However, necrosis is also characterized by the large reduction in ATP levels [53]. High levels of ATP, such as that observed in this work, are generally associated with apoptosis, and may therefore occur by stimulating mitochondrial production or glycolytic reactions [55]. Despite this, no changes were observed in mitochondrial membrane potential.

Excess ROS can damage important macromolecules, including lipids, nucleic acids, and proteins [56]. We observed an intense dose-dependent lipid peroxidation, which may be associated with disruption of the plasma membrane in PC3 cells. Pre-incubation with NAC consolidates this hypothesis. Because it is a source of sulfhydryl groups, NAC acts as an antioxidant and ROS scavenger [57]. Thus, treatment with NAC, besides inhibiting lipoperoxidation, was able to partially prevent lesions in the plasma membrane.

Therefore, the compound GSCB42 showed antitumor activity in PC3 cells leading to cell death, possibly due to oxidative stress.

4. Conclusion

Screening of a series of N-containing nitrogen heterocyclic compounds identified new compounds with tumor activity. GSCB42, GSCB46 and GSCB47 exhibit better results. Unfortunately, GSCB42 shows no potential for inhibition of metastasis, since it did not prevent cell migration in *in vitro* assay. Oxidative stress appears to be involved in GSCB42-induced cell death, as well as early plasma membrane rupture. However further studies are needed to clarify the cell death pathway. In addition, further studies involving the modification of substituents may increase the potential of the compound and increase its selectivity.

References

1. World Health Organization. Cancer. Available online: <http://www.who.int/mediacentre/factsheets/fs297/en/> (accessed on 12 August 2018).

2. The Cancer Atlas. The burden. Available online: <http://canceratlas.cancer.org/the-burden/> (accessed on 12 August 2018).
3. Kumar, B.; Koul, S.; Khandrika, L.; Meacham, R.B.; Koul, H.K. Oxidative stress is inherent in prostate cancer cells and mediates aggressive phenotype. *Cancer Res.* **2008**, *68*, 1777-1785. DOI: 10.1158/0008-5472.CAN-07-5259.
4. Denmeade, S.R.; Isaacs, J.T. A history of prostate cancer treatment. *Nat. Rev. Cancer.* **2002**, *2*, 389-396. DOI: 10.1038/nrc801.
5. Rivera, M.; Ramos, Y.; Rodríguez-Valentín, M.; López-Acevedo, S.; Cubano, L.A.; Zou, J.; Zhang, Q.; Wang, G.; Boukli, N.M. Targeting multiple pro-apoptotic signaling pathways with curcumin in prostate cancer cells. *Plos One.* **2017**, *12*, e0179587. DOI: 10.1371/journal.pone.0179587.
6. Baciarello, G.; Gizzi, M.; Fizazi, K. Advancing therapies in metastatic castration-resistant prostate cancer. *Expert Opinion on Pharmacotherapy.* **2018**, 1-8. DOI: 10.1080/14656566.2018.1527312.
7. Dolezal, M.; Cmedlova, P.; Palek, L.; Vinsova, J.; Kunes, J.; Buchta, V.; Jampilek, J.; Kralova, K. Synthesis and antimycobacterial evaluation of substituted pyrazinecarboxamides. *Eur. J. Med. Chem.* **2008**, *43*, 105-1113. DOI: 10.1016/j.ejmech.2007.07.013.
8. Foks, H.; Balewski, L.; Gobis, K.; Dabrowska-Szponar, M.; Wisniewska, K. Studies on pyrazine derivatives LII: antibacterial and antifungal activity of nitrogen heterocyclic compounds obtained by pyrazinamidrazone usage. *Heteroat. Chem.* **2012**, *23*, 49-58. DOI: 10.1002/hc.20751.
9. Verbitskiy, E.V.; Slepukhin, P.A.; Kravchenko, M.A.; Skornyakov, S.N.; Evstigneeva, N.P.; Kungurov, N.V.; Zil'berberg, N.V.; Rusinov, G.L.; Chupakhin, O.N., Charushin, V.N. Synthesis, antimycobacterial and antifungal evaluation of some new 1-ethyl-5-(hetero) aryl-6-styryl-1, 6-dihydropyrazine-2, 3-dicarbonitriles. *Bioorg. Med. Chem. Lett.* **2015**, *25*, 524-528. DOI: 10.1016/j.bmcl.2014.12.025.
10. Wu, H.M.; Zhou, K.; Wu, T.; Cao, Y.G. Synthesis of Pyrazine-1, 3-thiazine Hybrid Analogues as Antiviral Agent Against HIV-1, Influenza A (H1N1), Enterovirus 71 (EV 71), and Coxsackievirus B3 (CVB 3). *Chem. Biol. Drug Des.* **2016**, *88*, 411-421. DOI: 10.1111/cbdd.12769.
11. Jandourek, O.; Tauchman, M.; Paterova, P.; Konecna, K.; Navratilova, L.; Kubicek, V.; Holas, O.; Zitko, J. Dolezal, M. Synthesis of Novel Pyrazinamide Derivatives Based on 3-Chloropyrazine-2-carboxamide and Their Antimicrobial Evaluation. *Molecules.* **2017**, *22*, 223. DOI: 10.3390/molecules22020223.
12. Matthew, A.N.; Zephyr, J.; Hill, C.J.; Jahangir, M.; Newton, A.; Petropoulos, C.J.; Huang, W.; Kurt-Yilmaz, N.; Schiffer, C.; Ali, A. Hepatitis C virus NS3/4A protease inhibitors incorporating flexible P2 quinoxalines target drug resistant viral variants. *J. Med. Chem.* **2017**, *60*, 5699-5716. DOI: 10.1021/acs.jmedchem.7b00426.
13. Semelková, L.; Janošcová, P.; Fernandes, C.; Bouz, G.; Jand'ourek, O.; Konečná, K.; Paterová, P.; Navrátilová, L.; Kuneš, J.; Doležal, M.; Zitko, J. Design,

- Synthesis, Antimycobacterial Evaluation, and In Silico Studies of 3-(Phenylcarbamoyl)-pyrazine-2-carboxylic Acids. *Molecules*. **2017**, *22*, 1491. DOI: %2010.3390/molecules22091491.
14. Cogo, J.; Kaplum, V.; Sangi, D.P.; Ueda-Nakamura, T.; Corrêa, A.G.; Nakamura, C.V. Synthesis and biological evaluation of novel 2, 3-disubstituted quinoxaline derivatives as antileishmanial and antitrypanosomal agents. *Eur. J. Med. Chem.* **2015**, *90*, 107-123. DOI: 10.1016/j.ejmech.2014.11.018.
 15. Patil, S.R.; Asrondkar, A.; Patil, V.; Sangshetti, J.N.; Khan, F.A.K.; Damale, M.G.; Patil, R.H.; Bobade, A.S.; Shinde, D.B. Antileishmanial potential of fused 5-(pyrazin-2-yl)-4H-1, 2, 4-triazole-3-thiols: Synthesis, biological evaluations and computational studies. *Bioorg. Med. Chem Lett.* **2017**, *27*, 3845-3850. DOI: 10.1016/j.bmcl.2017.06.053.
 16. Quiliano, M.; Pabón, A.; Ramirez-Calderon, G.; Barea, C.; Deharo, E.; Galiano, S.; Aldana, I. New hydrazine and hydrazide quinoxaline 1, 4-di-N-oxide derivatives: In silico ADMET, antiplasmodial and antileishmanial activity. *Bioorg. Med. Chem. Lett.* **2017**, *27*, 1820-1825. DOI: 10.1016/j.bmcl.2017.02.049.
 17. Shen, J.; Li, X.; Zhang, Z.; Luo, J.; Long, H.; Tu, Z.; Zhou, X., Ding, K.; Lu, X. 3-aminopyrazolopyrazine derivatives as spleen tyrosine kinase inhibitors. *Chem. Biol. Drug Des.* **2016**, *88*, 690-698. DOI: 10.1111/cbdd.12798.
 18. Pandey, D.K.; Devadoss, T.; Modak, N.; Mahesh, R. Antidepressant & anxiolytic activities of N-(pyridin-3-yl) quinoxalin-2-carboxamide: A novel serotonin type 3 receptor antagonist in behavioural animal models. *Indian J. Med. Res.* **2016**, *144*, 614-621. DOI: 10.4103/0971-5916.200893.
 19. Ibrahim, M.K.; Eissa, I.H.; Abdallah, A.E.; Metwaly, A.M.; Radwan, M.M.; ElSohly, M.A. Design, synthesis, molecular modeling and anti-hyperglycemic evaluation of novel quinoxaline derivatives as potential PPAR γ and SUR agonists. *Bioorg. Med. Chem.* **2017**, *25*, 1496-1513. DOI: 10.1016/j.bmc.2017.01.015.
 20. Ghosh, A.; Sengupta, A.; Seerapu, G.P.K.; Nakhi, A.; Ramarao, E.V.V.S.; Bung, N.; Bulusu, G.; Pal, M.; Haldar, D. A novel SIRT1 inhibitor, 4bb induces apoptosis in HCT116 human colon carcinoma cells partially by activating p53. *Biochem. Biophys. Res. Commun.* **2017**, *488*, 562-569. DOI: 10.1016/j.bbrc.2017.05.089.
 21. Gu, W.; Wang, S.; Jin, X.; Zhang, Y.; Hua, D.; Miao, T.; Tao, X., Wang, S. Synthesis and evaluation of new quinoxaline derivatives of dehydroabietic acid as potential antitumor agents. *Molecules*. **2017**, *22*, 1154. DOI: 10.3390/molecules22071154.
 22. Xu, S.; Sun, C.; Chen, C.; Zheng, P.; Zhou, Y.; Zhou, H.; Zhu, W. Synthesis and Biological Evaluation of Novel 8-Morpholinoimidazo [1, 2-a] pyrazine Derivatives Bearing Phenylpyridine/Phenylpyrimidine-Carboxamides. *Molecules*. **2017**, *22*, 310. DOI: 10.3390/molecules22020310.
 23. Zhang, Y.; Liu, H.; Zhang, Z.; Wang, R.; Liu, T.; Wang, C.; Ma, Y.; Ai, J.; Zhao, D.; Shen, J.; Xiong, B. Discovery and Biological Evaluation of a Series of

- Pyrrolo[2, 3-b]pyrazines as Novel FGFR Inhibitors. *Molecules*. **2017**, *22*, 583. DOI: 10.3390/molecules22040583.
24. Liang, C.C.; Park, A.Y.; Guan, J.L. In vitro scratch assay: a convenient and inexpensive method for analysis of cell migration in vitro. *Nat. Protoc.* **2007**, *2*, 329–333. DOI: 10.1038/nprot.2007.30.
 25. Souza, R.P.; Bonfim-Mendonça, P.S.; Gimenes, F.; Ratti, B.A.; Kaplum, V.; Bruschi, M.L.; Nakamura, C.V.; Silva, S.O.; Maria-Engler, S.S.; Consolaro, M.E.L. Oxidative stress triggered by apigenin induces apoptosis in a comprehensive panel of human cervical cancer-derived cell lines. *Oxid. Med. Cell. Long.* **2017**, 1512745. DOI: 10.1155/2017/1512745.
 26. Ghanbarimasir, Z.; Bekhradnia, A.; Morteza-Semnani, K.; Rafiei, A.; Razzaghi-Asl, N.; Kardan, M. Design, synthesis, biological assessment and molecular docking studies of new 2-aminoimidazole-quinoxaline hybrids as potential anticancer agents. *Spectrochim. Acta A Mol. Biomol. Spectrosc.* **2017**, *194*, 21-35. DOI: /10.1016/j.saa.2017.12.063.
 27. Galal, S.A.; Abdelsamie, A.S.; Soliman, S.M.; Mortier, J.; Wolber, G.; Ali, M.M.; Tokuda, H.; Suzuki, N.; Lida, A.; Ramadan, R.A.; Diwani, H.I. Design, synthesis and structure–activity relationship of novel quinoxaline derivatives as cancer chemopreventive agent by inhibition of tyrosine kinase receptor. *Eur. J. Med. Chem.* **2013**, *69*, 115-124. DOI: 10.1016/j.ejmech.2013.07.049.
 28. Yang, J.; Amiri, K.I.; Burke, J.R.; Schmid, J.A.; Richmond, A. BMS-345541 targets inhibitor of κ B kinase and induces apoptosis in melanoma: involvement of nuclear factor κ B and mitochondria pathways. *Clin. Cancer Res.* **2006**, *12*, 950-960. DOI: 10.1158/1078-0432.CCR-05-1220.
 29. Amin, K.M.; Ismail, M.M.; Noaman, E.; Soliman, D.H.; Ammar, Y.A. New quinoxaline 1, 4-di-N-oxides. Part 1: Hypoxia-selective cytotoxins and anticancer agents derived from quinoxaline 1, 4-di-N-oxides. *Bioorg. Med. Chem.* **2006**, *14*, 6917-6923. DOI: 10.1016/j.bmc.2006.06.038.
 30. Zhao, X.; Xia, C.; Wang, X.; Wang, H.; Xin, M; Yu, L.; Liang, Y. Cyclophilin J PPIase Inhibitors Derived from 2, 3-Quinoxaline-6 Amine Exhibit Antitumor Activity. *Front. Pharmacol.* **2018**, *9*, 126. DOI: 10.3389/fphar.2018.00126.
 31. Gomtsyan, A. Heterocycles in drugs and drug discovery. *Chem. Heterocycl. Compd.* **2012**, *48*, 7-10. DOI: 10.1007/s10593-012-0960-z.
 32. Pereira, J.A.; Pessoa, A.M.; Cordeiro, M.N.D.; Fernandes, R.; Prudêncio, C.; Noronha, J.P.; Vieira, M. Quinoxaline, its derivatives and applications: a state of the art review. *Eur. J. Med. Chem.* **2015**, *97*, 664-672. DOI: 10.1016/j.ejmech.2014.06.058.
 33. Strober, W. Trypan blue exclusion test of cell viability. *Curr. Protoc. Immunol.* **1997**, *21*, A-3B. DOI: 10.1002/0471142735.ima03bs21.
 34. Weyermann, J.; Lochmann, D.; Zimmer, A. A practical note on the use of cytotoxicity assays. *Int. J. Pharm.* **2006**, *288*, 369-376. DOI: 10.1016/j.ijpharm.2004.09.018.

35. Fotakis, G.; Timbrell, J.A. In vitro cytotoxicity assays: comparison of LDH, neutral red, MTT and protein assay in hepatoma cell lines following exposure to cadmium chloride. *Toxicol. Lett.* **2006**, *160*, 171-177. DOI: 10.1016/j.toxlet.2005.07.001.
36. Noolvi, M.N.; Patel, H.M.; Bhardwaj, V.; Chauhan, A. Synthesis and in vitro antitumor activity of substituted quinazoline and quinoxaline derivatives: search for anticancer agent. *Eur. J. Med. Chem.* **2011**, *46*, 2327-2346. DOI: 10.1016/j.ejmech.2011.03.015.
37. Liang, C.C.; Park, A.Y.; Guan, J.L. In vitro scratch assay: a convenient and inexpensive method for analysis of cell migration in vitro. *Nat. Protoc.* **2007**, *2*, 329. DOI: 10.1038/nprot.2007.30.
38. Jonkman, J.E.; Cathcart, J.A.; Xu, F.; Bartolini, M.E.; Amon, J.E. An introduction to the wound healing assay using live-cell microscopy. *Cell Adh. Migr.* **2014**, *8*, 440-451. DOI: 10.4161/cam.36224.
39. Das, T.P.; Suman, S.; Damodaran, C. Induction of reactive oxygen species generation inhibits epithelial–mesenchymal transition and promotes growth arrest in prostate cancer cells. *Mol. Carcinog.* **2014**, *53*, 537-547. DOI: 10.1002/mc.22014.
40. Zhou, M.; Diwu, Z.; Panchuk-Voloshina, N.; Haugland, R.P. A stable nonfluorescent derivative of resorufin for the fluorometric determination of trace hydrogen peroxide: applications in detecting the activity of phagocyte NADPH oxidase and other oxidases. *Anal. Biochem.* **1997**, *253*, 162-168. DOI: 10.1006/abio.1997.2391.
41. Votyakova, T.V.; Reynolds, I.J. Detection of hydrogen peroxide with Amplex Red: interference by NADH and reduced glutathione auto-oxidation. *Arch. Biochem. Biophys.* **2004**, *431*, 138-144. DOI: 10.1016/j.abb.2004.07.025.
42. Zhao, B.; Summers, F.A.; Mason, R.P. Photooxidation of Amplex Red to resorufin: implications of exposing the Amplex Red assay to light. *Free Radical Biol. Med.* **2012**, *53*, 1080-1087. DOI: 10.1016/j.freeradbiomed.2012.06.034.
43. Rahman, I.; Kode, A.; Biswas, S.K. Assay for quantitative determination of glutathione and glutathione disulfide levels using enzymatic recycling method. *Nat. Protoc.* **2006**, *1*, 3159-3165. DOI: 10.1038/nprot.2006.378.
44. Winther, J.R.; Thorpe, C. Quantification of thiols and disulfides. *BBA Gen. Subjects.* **2014**, *1840*, 838-846. DOI: 10.1016/j.bbagen.2013.03.031.
45. Abuja, P.M.; Albertini, R. Methods for monitoring oxidative stress, lipid peroxidation and oxidation resistance of lipoproteins. *Clin. Chim. Acta.* **2001**, *306*, 1-17. DOI: 10.1016/S0009-8981(01)00393-X.
46. Okimoto, Y.; Watanabe, A.; Niki, E.; Yamashita, T.; Noguchi, N. A novel fluorescent probe diphenyl-1-pyrenylphosphine to follow lipid peroxidation in cell membranes. *FEBS Lett.* **2000**, *474*, 137-140. DOI: 10.1016/S0014-5793(00)01587-8.
47. Sinha, K.; Das, J.; Pal, P.B.; Sil, P.C. Oxidative stress: the mitochondria-dependent and mitochondria-independent pathways of apoptosis. *Arch. Toxicol.* **2013**, *87*, 1157-1180. DOI: 10.1007/s00204-013-1034-4.

48. Ly, J.D.; Grubb, D.R.; Lawen, A. The mitochondrial membrane potential ($\Delta\psi_m$) in apoptosis; an update. *Apoptosis*. **2003**, *8*, 115-128. DOI: 10.1023/A:1022945107762.
49. Scaduto Jr, R.C.; Grotyohann, L.W. Measurement of mitochondrial membrane potential using fluorescent rhodamine derivatives. *Biophys. J.* **1999**, *76*, 469-477. DOI: 10.1016/S0006-3495(99)77214-0.
50. Zhao, L.; Wu, T.W.; Brinton, R.D. Estrogen receptor subtypes alpha and beta contribute to neuroprotection and increased Bcl-2 expression in primary hippocampal neurons. *Brain Res.* **2004**, *1010*, 22-34. DOI: 10.1016/j.brainres.2004.02.066.
51. Krysko, D.V.; Berghe, T.V.; D'Herde, K.; Vandenabeele, P. Apoptosis and necrosis: detection, discrimination and phagocytosis. *Methods*. **2008**, *44*, 205-221. DOI: 10.1016/j.ymeth.2007.12.001.
52. Halliwell, B.; Chirico, S. Lipid peroxidation: its mechanism, measurement, and significance. *Am J Clin Nutr.* **1993**, *57*, 715-725. DOI:10.1093/ajcn/57.5.715s.
53. Pierzyńska-Mach, A.; Janowski, P.A.; Dobrucki, J.W. Evaluation of acridine orange, LysoTracker Red, and quinacrine as fluorescent probes for long-term tracking of acidic vesicles. *Cytom. Part A.* **2014**, *85*, 729-737. DOI: 10.1002/cyto.a.22495.
54. Nikolettou, V.; Markaki, M.; Palikaras, K.; Tavernarakis, N. Crosstalk between apoptosis, necrosis and autophagy. *BBA Mol. Cell Res.* **2013**, *1833*, 3448-3459. DOI: 10.1016/j.bbamcr.2013.06.001.
55. Zamaraeva, M.V.; Sabirov, R.Z.; Maeno, E.; Ando-Akatsuka, Y.; Bessonova, S.V.; Okada, Y. Cells die with increased cytosolic ATP during apoptosis: a bioluminescence study with intracellular luciferase. *Cell Death Differ.* **2005**, *12*, 1390-1397. DOI: 10.1038/sj.cdd.4401661.
56. Birben, E.; Sahiner, U. M.; Sackesen, C.; Erzurum, S.; Kalayci, O. Oxidative Stress and Antioxidant Defense. *World Allergy Organ J.* **2012**, *5*, 9-19. DOI:10.1097/wox.0b013e3182439613.
57. Zafarullah, M.; Li, W. Q.; Sylvester, J.; Ahmad, M. Molecular mechanisms of N-acetylcysteine actions. *Cell Mol Life Sci.* **2003**, *60*, 6-20. DOI: 10.1007/s000180300001.